第42卷 第8期
2014年8月

燃 料 化 学 学 报
Journal of Fuel Chemistry and Technology

Vol. 42 No. 8
Aug. 2014

文章编号：0253-2409(2014)08-0922-10

Chemical-looping gasification of biomass in a 10 kW_{th} interconnected fluidized bed reactor using Fe_2O_3/Al_2O_3 oxygen carrier

HUSEYIN Sozen, WEI Guo-qiang, LI Hai-bin, HE Fang, HUANG Zhen
(*CAS Key Laboratory of Renewable Energy, Guangzhou Institute of Energy Conversion, Chinese Academy of Sciences (CAS), Guangzhou* 510640, *China*)

Abstract: The aim of this research is to design and operate a 10 kW hot chemical-looping gasification (CLG) unit using Fe_2O_3/Al_2O_3 as an oxygen carrier and saw dust as a fuel. The effect of the operation temperature on gas composition in the air reactor and the fuel reactor, and the carbon conversion of biomass to CO_2 and CO in the fuel reactor have been experimentally studied. A total 60 h run has been obtained with the same batch of oxygen carrier of iron oxide supported with alumina. The results show that CO and H_2 concentrations are increased with increasing temperature in the fuel reactor. It is also found that with increasing fuel reactor temperature, both the amount of residual char in the fuel reactor and CO_2 concentration of the exit gas from the air reactor are degreased. Carbon conversion rate and gasification efficiency are increased by increasing temperature and H_2 production at 870 ℃ reaches the highest rate. Scanning electron microscopy (SEM), X-ray diffraction (XRD) and BET-surface area tests have been used to characterize fresh and reacted oxygen carrier particles. The results display that the oxygen carrier activity is not declined and the specific surface area of the oxygen carrier particles is not decreased significantly.

Keywords: chemical-looping gasification; hot model; biomass; Fe_2O_3/Al_2O_3; dual circulating fluidized bed
CLC number: YQ016 **Document code**: A

Carbon dioxide emitted from fossil fuel power plants accounts for roughly 20% of the greenhouse effect and climate change[1]. There are some novel technologies being developed to reduce and capture the CO_2 emissions from conventional power plants. Chemical-looping combustion (CLC) is one of the techniques used to combine fuel combustion and CO_2 capture at the same time without any need of air separation unit. Chemical-looping combustion (CLC) is a new combustion technique where an oxygen carrier is used to transfer oxygen from the air reactor to the fuel reactor, omitting direct contact between air and fuel. Thus, CO_2 and H_2O are inherently separated from the other noncondensible components of the flues gas, such as N_2 and unused O_2[2,3]. Then, the CO_2 can be recovered by condensing the vapor of water without energy penalty and the dewatered CO_2 can be captured and sequestrated or/and can be used for other applications[4]. The properties of the oxygen carrier are important for the experiments of the process of CLC, and an oxygen carrier should have high reactivity, high oxygen transport capacity, high resistance to attrition, and cheap and environmentally friendly. Chemical-looping reforming (CLR) or chemical-looping gasification (CLG) uses the same basic principles as CLC with the main difference that the final products in CLR or CLG are synthesis gas (H_2 and CO) instead of full combustion final products like CO_2 and H_2O, and heat[5].

Different metal oxides as oxygen carrier, such as Ni, Cu, Fe, Mn, Co and some mixed metal oxides have been proposed for CLC recently. Generally, Ni and its corresponding oxide show relatively higher oxidation and reduction rates than other metals but it is an expensive and hazardous candidate. Copper oxide indicates high reactivity in the redox reaction with air and fuel in CLC tests. But CuO has agglomeration and softening problem because of its low melting point. A further problem with CuO at high temperatures (870 ℃) is that CuO can decompose to Cu_2O that can lower oxygen capacity for oxidizing fuel. Oxides of Mn and Co have showed a rather poor reactivity[6].

Iron oxide is cheaper than CuO and NiO and environmentally friendly. All iron compounds have higher level of melting points and can stand cyclic reactions in the fuel and air reactor of CLC[7]. According to the thermodynamic analysis for iron oxygen carriers, the complete fuel conversion to CO_2 and H_2O is only possible when Fe_2O_3 is partially reduced to Fe_3O_4[8]. Iron oxide is still an attractive

---

Received date: 2014-04-11; **Received in revised form**: 2014-05-30.

Foundhtion item: Supported by the National Natural Science Foundation of China (51076154); National Key Technology Research & Development Program of 12 th Five-year of China (2011BAD15B05).

Corresponding author: E-mail: lihb@ms.giec.ac.cn.

oxygen carrier for the industrial application of CLC or CLG as its easy availability and low price even the capacity of Fe_2O_3 for transferring oxygen is only 0.5 mol of O_2 delivered per 3 mol of Fe_2O_3. For the mentioned advantages, Fe_2O_3 on Al_2O_3 support has been selected as oxygen carrier for the present work.

Gaseous fuels such as methane, hydrogen, and syngas from coal gasification and solid fuels like coal, pet coke, char and biomass can be use as fuel in CLC or CLG[9]. Most of the researches on oxygen carrier have been performed in a laboratory fluidized bed reactor and thermo gravimetric analyzers (TGA), and few of them studied on dual or interconnected fluidized bed reactor with solid fuels. The oxygen carrier reactivity should cover number of cycles, and the reactivity of the oxygen carrier should stand to thermal stresses and accumulative chemical reactions during the cyclic operations.

Limited number of studies can be seen on using oxygen carriers for CLC with biomass solid fuel in a continuous CLC or CLG reactor in the literature. For the quoted two-stage dual fluidized bed gasification (T-DFBG) devises, Xua et al[10] has studied the use of a two-stage fluidized bed (TFB) to replace the single-stage bubbling fluidized bed gasifier involved in the normally encountered dual fluidized bed gasification (N-DFBG) systems, gasifying dry coffee grounds in two 5.0 kg/h. Shen et al[11] has experimented on the CLC of biomass in a 10 kWth reactor with iron oxide as an oxygen carrier. A total 30 h of test was achieved with the same batch of iron oxide oxygen carrier. The results showed that the CO production from biomass gasification with CO_2 was more temperature dependent than the CO oxidation with iron oxide in the fuel reactor, and an increase in the fuel reactor temperature produced a higher increase for the CO production from biomass gasification than for the oxidation of CO by iron oxide. Zhang et al[12] has studied on simulation of methanol synthesis via H_2-rich biomass-derived syngas from straw biomass gasification in interconnected fluidized beds. In the case of $CaCO_3$ catalysis, the effects of operating parameters, including gasification temperature and pressure, steam/biomass ratio, and liquefaction temperature and pressu on the methanol yield were analyzed. Acharya et al[13] has investigated on H_2 production process employing fluidized-bed technology from agricultural biomass sawdust with in situ CO_2 capture and sorbent regeneration. The system efficiency of the chemical-looping gasification process at an ideal scenario was found to be 87.49% with biomass as fuel. Xie et al[14] has experimented for the catalytic performances of natural Ca-based catalysts (dolomite and limestone) and synthetic Ca-based catalysts, which have been used for improving biomass rice straw steam gasification in a circulating spout-fluid bed reactor. Li et al[15] has presented on the biomass direct chemical looping (BDCL) process, an alternative process, which has the potential to thermo chemically convert biomass to hydrogen and/or electricity with high efficiency. Process simulation has been investigated by ASPEN Plus, and then data were obtained from the multistage model. Hybrid poplar as biomass fuel and oxygen carrier of 66.2% Fe_2O_3 and 33.8% SiC by weight were used during the study. Gnanapragasam et al[16] has reported on the performance of four different coals and biomass with iron oxide-based direct chemical looping combustion system, the impact of fuel blend (mix. of coal and biomass) on hydrogen production was compared. When biomass was blended with 20% coal by mass, 10% additional hydrogen was produced. Gu et al[17] has studied on chemical looping combustion of biomass and coal conducted in a 1 kW_{th} continuous reactor with Australian iron ore as a oxygen carrier. The effect of temperature on gas composition of both the fuel reactor and the air reactor, conversion efficiency of carbonaceous gases, carbon capture efficiency and oxide oxygen fraction were investigate.

Virginie et al[18] has provided that the Fe/olivine catalyst effectiveness regarding tar primary reduction during biomass gasification in dual fluidized beds. It was found that Fe/olivine materials had a double effect on tar destruction. On the one hand, they were acted as a catalyst for tar and hydrocarbon reforming. Furthermore, they could act as an oxygen carrier that transfers oxygen from the combustor to the gasifier, and part of the oxygen is used to burn volatile compounds. The catalyst was fairly stable because the result was confirmed during 48 h continuous operation. Song et al[19] has investigated hydrogen production from biomass gasification in a laboratory scale apparatus of interconnected fluidized beds. The effects of gasifier temperature and steam/biomass ratio on the composition of hydrogen-rich gas, carbon gasification of biomass, carbon combustion of biomass, carbon utilization of biomass, tar content and hydrocarbons were discussed. Mendiara et al[20] has studied biomass combustion in a continuous CLC unit using pine wood as fuel and iron ore as an oxygen carrier. High carbon captures (>95%) were achieved in the interval 880 ~ 915 ℃ using both steam and CO_2 as gasifying agents. Tar compounds were detected at the fuel reactor outlet. After 78 h continuous operation, no change was detected in the physical and chemical properties of the oxygen carrier particles. Gu et al[21] has prepared biomass-to-synthetic natural gas (SNG) using calcium looping gasification (CLG) with CaO sorbent (CLG-SNG) via thermo chemical methods. Interconnected fluidized beds were adopted for repeated carbonation/calcination cycles of CaO sorbents in the gasification unit. A process simulation was conducted based on the chemical equilibrium method using the Aspen Plus. Then, the effects of some key variables on the thermodynamic performances, such as the gas composition, yield of SNG (YSNG), cold gas efficiency (η cold), the overall energy efficiency (η), energy efficiency (ψ) of the process, and the unit power consumption (WSNG) were investigated.

Biomass is called as any organic matter, which is available on a renewable basis, including agricultural crops, plants and agricultural wastes and residues, wood and wood wastes and residues, animal wastes, municipal wastes, and aquatic plants. This renewable resource can be converted into electricity, chemicals, hydrogen, heat and liquid fuels. Biomass conversion is less carbon and pollutant intensive when compared to fossil based fuels. Furthermore, these renewable matters are abundantly available and widely distributed in the any part of the World. As source of renewable clean energy, biomass can achieve the goal of CO_2 zero-emissions and reduce the climate change and greenhouse effect in the industrial and power utilization. Nowadays, biomass development and employment in energy production has gained great attention from all over the world[22]. Sawdust of pine has been selected as biomass fuel in this work for the above mentioned reasons.

CLG rather than CLC in this experiment is employed as electricity prices in China is nearly fixed and there are lots of imports on transport fuels and natural gas. When pure and high quality H_2 and CO are mixed as syngas, it is able to produce FT gasoline and diesel, and synthetic methane.

The performance of chemical-looping gasification (CLG) of biomass as fuel has been experimentally investigated in the 10 kW_{th} reactor with Fe_2O_3/Al_2O_3 (70% :30% by weight) as an oxygen carrier in the present work. A total 60 h cyclic test has been achieved with the same batch of oxygen carrier. The effect of the fuel reactor temperature on produced gas composition of the fuel reactor and the air reactor, and the conversion of biomass carbon to gases in the fuel reactor has been experimentally reported. Scanning electron microscopy (SEM), X-ray diffraction (XRD) and BET-surface area tests have been used to characterize fresh and reacted or used oxygen carrier particles.

1 Thermodynamics analysis

In the continuous tests, the reactions between the reduced iron based oxygen carriers with the combustion air in the air reactor are as follows:

$$4Fe_3O_4+O_2\rightarrow 6Fe_2O_3 \quad (1)$$

$$4FeO+O_2\rightarrow 2Fe_2O_3 \quad (2)$$

When the biomass is feeded into the bed materials of the fuel reactor, an intensive contact between hot oxygen carrier particles and biomass will happen, following by the intense exchange of heat. The biomass is immediately heated up to the bed temperature in the fuel reactor. Then, devolatilization and gasification of biomass has taken place in the lower zone of the bubbling fluidized bed. The main reactions probably are pyrolysis and gasification of biomass and boudouard in the fuel reactor:

$$C_nH_{2m}O_x\rightarrow \text{char} + \text{tar} + \text{syngas}\ (CO,\ H_2,\ CO_2,\ CH_4,\ C_nH_{2m}) \quad (3)$$

$$\text{Boudouard: } C+CO_2\rightarrow 2CO \quad (4)$$

The main reduction reactions of oxygen carrier particle with pyrolytic and syngas products of biomass are presented below in the fuel reactor[11,23]:

$$CO + 3Fe_2O_3\rightarrow CO_2 + 2Fe_3O_4 \quad (5)$$

$$CO + Fe_2O_3\rightarrow CO_2 + 2FeO \quad (6)$$

$$CO + Fe_3O_4\rightarrow CO_2 + 3FeO \quad (7)$$

$$CO + FeO\rightarrow CO_2+Fe \quad (8)$$

$$H_2 + 3Fe_2O_3\rightarrow H_2O + 2Fe_3O_4 \quad (9)$$

$$H_2 + Fe_2O_3\rightarrow H_2O + 2FeO \quad (10)$$

$$H_2 + Fe_3O_4\rightarrow H_2O + 3FeO \quad (11)$$

$$H_2 + FeO\rightarrow H_2O + Fe \quad (12)$$

$$CH_4 + 3Fe_2O_3\rightarrow 2H_2 + CO + 2Fe_3O_4 \quad (13)$$

$$CH_4 + 4Fe_2O_3\rightarrow 2H_2O + CO_2+8FeO \quad (14)$$

$$CH_4 + 4Fe_3O_4\rightarrow 2H_2O + CO_2+12FeO \quad (15)$$

$$CH_4 + 4FeO \rightarrow 2H_2O + CO_2+4Fe \quad (16)$$

$$C + 3\ Fe_2O_3\rightarrow CO + 2\ Fe_3O_4 \quad (17)$$

$$C + 2\ Fe_2O_3\rightarrow CO_2 + 4FeO \quad (18)$$

Therefore, these reactions occur sequentially and simultaneously during biomass pyrolysis and gasification in the presence of oxygen carriers. The final products of biomass gasification are determined by the interaction of a couple of above mentioned heterogeneous reactions.

Obviously, the reduction of iron oxygen carrier by gas intermediates would accelerate the process of biomass gasification. In addition, the tar would be decomposed to small molecular weight gases in the presence of iron oxide as follows[24]:

$$\text{Tar} \rightarrow H_2+CO+\text{hydrocarbon} \quad \Delta H > 0 \quad (19)$$

In comparison to traditional biomass gasification, the chemical reactions in the process of CLG are more complicated due to the presence of oxygen carrier. Biomass gasification and oxygen carrier reduction with biomass syngas occur simultaneously in CLG. The other reactions involved in the biomass gasification have relation with water produced during the oxygen carrier reduction by syngas components. Similar reactions also occur when steam is used as fluidizing gas. These reactions are shown as follows：

Water gas：$C + H_2O(g) \rightarrow H_2 + CO$ (20)

Water-gas shift：$CO + H_2O(g) \rightarrow H_2 + CO_2$ (21)

Steam reforming：$CH_4 + H_2O(g) \rightarrow 3H_2 + CO$ (22)

The flue gas exhausting from in the fuel reactor is gas mixture of H_2， CO_2， CO and CH_4. The particles of reduced oxygen carrier in the bubbling fluidized bed return back to the air reactor via a lower loop seal.

2　Experimental

2.1　Materials

Sawdust of pine selected from Guangdong province（China）is used as fuel in the tests. The sample size is ranged 250～425 mm. It has been dried for 8 h at 105 ℃ before experiment. The ultimate analysis of the pine（*w*%，dry basis）is 46.44% carbon，6.21% hydrogen，0.05% nitrogen，0.01% sulfur and 47.29% oxygen（by difference）. Its lower heating value was 18.707 HHV（kJ/kg，db）. The proximate analysis of the pine（*w*%，dry basis）was 8.39% moisture，84.31% volatile，6.88% fixed carbon and 0.42% ash. The oxygen carrier used in this work is Fe_2O_3/Al_2O_3 particles which are prepared by mechanical-mixing method.

2.1.1　Particle making and pelletization

The pelletization procedure involves two main steps. The first step involved is the powder preparation which processes the raw powders into a composite powder，and the second step is the actual pelletization of the powder. The powder preparation is performed by dry mixing 70% Fe_2O_3 powder and 30% Al_2O_3 as the support. The large pelletizer has a hopper which stores the powder and feeds into a rotary die set. The rotary die has a matching punch set which presses the powder into a pellet. The sticks of oxygen carrier are produced by sharing action of two screws which are interaction and mutual rotating with each other in the machine. After mixing is complete，the powder will have preparated into a wide range of sizes ranging from the desired particle size under 1 mm to up to 1 cm in diameter in reddish color. Then，they are calcinated in a small oven at 1 100 ℃ for 6 h. Thus，dried oxygen carriers with color changed in grayish are obtained. After drying，a manual system is used to grind and collect particles with an appropriate sizes. Thus，shaking sieves are used after hand selection. The process is repeated until the desired particle size is achieved.

2.2　Setup of interconnected fluidized bed reactor and procedure

The reactor is constructed with a 904 L stainless steel. The details of the reactor system are shown in Figure 1.

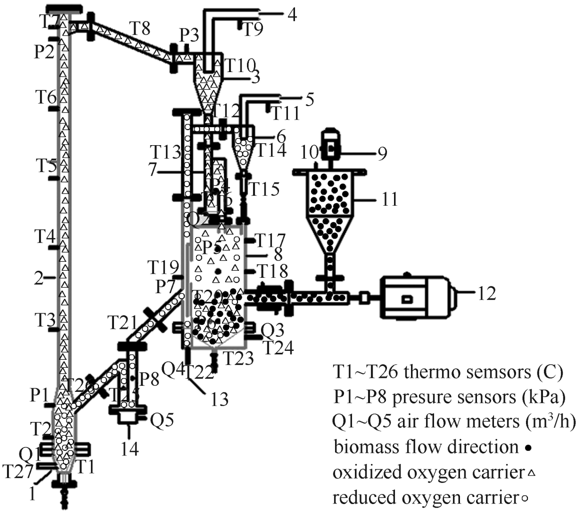

Figure 1　View of the reactor system of the hot model of laboratory unit in G. I. E. C.
1：air reactor gas flow；2：air reactor riser；
3：cyclone for air reactor；4：depleted gas；
5：synthesis gas；6：cyclone for fuel reactor；
7：upper loop seal；8：fuel reactor；9：biomass stirrer；
10：balance gas；11：biomass tank；12：biomass feeder；
13：fuel reactor gas flow；14：down loop seal

The experiments for chemical-looping gasification（CLG）of iron oxide and support with alumina as an oxygen carrier with biomass as fuel are conducted in a 10 kW$_{th}$ continuous reactor of interconnected fluidized beds as prototype which is consist of a fast fluidized bed as an air reactor，the first cyclone for depleted gas of the air reactor，a bubbling bed as fuel reactor，the second cyclones for synthesis gas of the fuel reactor and two loop seals. The one seal for entrance of the fuel reactor after the first cyclone is called upper loop seal and the other for exit of the fuel reactor to the air reactor is named down loop seal. The fast fluidized bed has a circular column of 50 mm in inner diameter and 2 100 mm in height with a perforated plate as an air distributor on the bottom of the reactor system. The bubbling bed has a similar shape with 150 mm in inner diameter and

500 mm in height with a perforated plate as an air distributor again. The two reactors are joined together by a rectangular loop seal with a cross section of 40×85 mm^2 and a height of 280 mm.

Strong solids mixing, recirculation of oxygen carriers and long residence time of biomass particles are very important for a high rate of carbon conversion efficiency in CLC or CLG. For this reason a bubbling fluidized bed is adopted for the fuel reactor. The fuel reactor has two parts, of which the major part is named as the reaction chamber and the minor one is the inner seal. The reaction chamber is used for biomass gasification and oxygen carrier reduction with syngas from biomass gasification. The inner seals having a height 320 (mm) allow movement of oxygen carriers from the reaction chamber in the fuel reactor to the down loop seal then to air reactor. At the same time, it prevents the by-passing of the flue gas from the air reactor to down loop seal and then to the fuel reactor. The down loop seal and the inner seals have roles in preventing gas leakage between the reactors. The oxygen carrier particles carried in the synthesis gas in the fuel reactor are separated by the second cyclone for the fuel reactor.

The heat required for the biomass gasification and oxygen carrier reduction with biomass syngas is achieved by means of the circulation of oxygen carrier particles between the air reactor and the fuel reactor. The biomass and reduction of oxygen carrier in the fuel reactor is an endothermic process, while the oxidization of oxygen carrier with air in the air reactor is exothermic one. As a result, there is a temperature difference between the fuel reactor and the air reactor. The oxygen carrier particles are heated up in the air reactor by exothermic reactions and then release given heat in the fuel reactor by circulation of oxygen carrier particles.

At the beginning of a test, the heating of the two reactor beds are electrically heated separately that supplies heat for start-up and compensated heat loss during a continuous operation. When the temperature of the two beds is electrically heated to 750 ℃, the air reactor is fluidized with air and the fuel reactor is fluidized with N_2 individually. Thermocouples and pressure transducer are located at different points of the reactor system as shown in Figure 1. Operating conditions can be rearranged at any time by the software on the computer and control panel. The outlets from the air reactor and fuel reactor are induced with suction pump to an ice-water cooler where the steam (if any) is condensed and removed. The reactant and synthesis gas product components are collected to gas bags for offline gas chromatograph analysis. All experiments are performed at atmospheric pressure and room temperature except the reactor system. Experimental conditions for 20 ~ 60 h long-term test with biomass (pine sawdust) as fuel are given in Table 1.

2.3 Oxygen carrier characterizations

The crystalline phases of the fresh and reacted oxides are analyzed by XRD (X' Pert PRO MPD) with Cu *Kα* radiation, operating voltage of 40 kV and current of 40 mA with a step size of 0.001 6 and the diffraction angle (2θ) scanned from 10° to 90°. The morphology of the Fe_2O_3/Al_2O_3-type oxides is studied by scanning electron microscopy (SEM) on a Hitachi S4800 instruments. The magnification of 15 000 (15 K) times is selected to analyze the surface micrographs of oxygen carrier. The BET surface area analyses sre experimentally investigated by N_2 physisorption using a Micromeritics ASAP 2010 instruments. The samples of Fe_2O_3/Al_2O_3-type oxides are degassed under vacuum at 493 K for 6 h before tests.

2.4 Data evaluation

The lower heating value (LHV, kJ/m^3) of the gas products is calculated by equation:

$$\mathrm{LHV} = 126\, v_{\mathrm{CO}} + 108\, v_{\mathrm{H_2}} + 359\, v_{\mathrm{CH_4}} + 635\, v_{\mathrm{C_2H}_m} \quad (23)$$

where v_{CO}, $v_{\mathrm{H_2}}$, $v_{\mathrm{CH_4}}$ and $v_{\mathrm{C_2H}_m}$ are the volume fractions of CO, H_2, CH_4 and C_2H_m in the product gas from fuel reactor, respectively.

Gas yield (G_v) is the volume of gas products under standard state generated from unit mass of biomass, which is calculated as:

$$G_v = v_{\mathrm{g}}/m_{\mathrm{b}} \quad (24)$$

where v_{g} is the volume of the gas products in standard state and m_{b} is the mass of the biomass.

Carbon conversion efficiency (η_{C}) is an important parameter to evaluate the performance of biomass gasification. It is defined as the proportion of the carbon converted into gaseous products to the total carbon in the biomass fed into the fuel reactor. The carbon conversion efficiency, η_{C}, is calculated by the following equation.

$$\eta_{\mathrm{C}} = 12 \times (v_{\mathrm{CO}} + v_{\mathrm{CO_2}} + v_{\mathrm{CH_4}} + 2v_{\mathrm{C_2H}_m}) \times G_v/22.4 \times (298/273) \times w \quad (25)$$

where G_v (m^3/kg) is the gas yield which is defined as the volume of gas products under standard state generated from unit mass of biomass, w is the carbon content of biomass and $v_{\mathrm{CO_2}}$, v_{CO}, $v_{\mathrm{CH_4}}$, and $v_{\mathrm{C_2H}_m}$ are the volume fractions of CO_2, CO, CH_4 and C_2H_m in the flue gas, respectively.

Table 1　Operational conditions of the interconnected fluidized bed reactor

No.	Operating parameter and design values	Value
1	thermal power /kW	10
2	biomass fuel as saw dust power /($kW \cdot h^{-1}$)	10
3	biomass fuel as saw dust stock particle size *d*/mm	250 ~ 425
4	stored biomass *m*/kg	4.8
5	biomass fuel flow/feeding rate (on dry basis) q_m/($kg \cdot h^{-1}$)	1.1
6	oxygen carrier (bed materials)	70% Fe_2O_3/30% Al_2O_3
7	total bed inventory *m*/kg	6.8
8	bed material particle size *d*/mm	0.25 ~ 0.425
9	oxygen carrier/biomass mass ratio	1:1.17
10	operating temperature *t*/℃	750 ~ 900
11	air inlet temperature *t*/℃	200
12	outlet gas temperature *t*/℃	178
13	outlet cold fuel gas temperature *t*℃	216
14	air flow mass controller for the air reactor *q*/($m^3 \cdot h^{-1}$)	12
15	N_2 flow mass controller for the fuel reactor *q*/($m^3 \cdot h^{-1}$)	6
16	N_2 flow mass controller for the upper loop seal *q*/($m^3 \cdot h^{-1}$)	2
17	N_2 flow mass controller for the down loop seal *q*/($m^3 \cdot h^{-1}$)	3
18	N_2 flow mass controller for the balance *q*/($m^3 \cdot h^{-1}$)	1
19	gas residence time in the fuel reactor (gasifier) *t*/s	2
20	biomass residence time in the fuel reactor (gasifier) *t*/s	7
21	operating pressure *p*/kPa	1.25
22	fluidization velocity of the fuel reactor /($m \cdot s^{-1}$)	1.1 ~ 1.5
23	fluidization velocity of the air reactor /($m \cdot s^{-1}$)	1.3 ~ 1.6
24	bed diameter of the fuel reactor *d*/mm	150
25	bed (max.) height of the fuel reactor *d*/mm	500
26	freeboard diameter of the air reactor *d*/mm	50
27	height of the air reactor *d*/mm	2 100
28	fluidization pipe diameter for T1-26 and P1-8 *d*/mm	6
29	fluidization pipe diameter for Q1 *d*/mm	22
30	fluidization pipe diameter for Q2-5 *d*/mm	12

Gasification efficiency (η) is defined as the ratio of the calorific value of the gas products from unit mass biomass gasification to the total calorific value of the unit mass of biomass. It is calculated as:

$$\eta = \mathrm{LHV} \cdot G_v / Q_b \qquad (26)$$

where G_v (m^3/kg) is the gas yield, LHV (kJ/m^3) and Q_b(kJ/kg) are the calorific value of the gas products and the biomass at room temperature, respectively.

CO selectivity s_{CO} (%) = (moles of CO produced)/(total moles of CO and CO_2 produced) × 100%　(27)

H_2 selectivity s_{H_2} (%) = (moles of H_2 produced)/(total moles of biomass used × 0.67) × 100%　(28)

3　Results and discussion

Long-term experiment of 20 ~ 60 h is established with the same batch of iron oxide particles without adding any fresh oxygen carrier particles into the hot system reactors and the feeding rate of biomass is kept as constant at 1.1 kg/h during the experiments. The air flow of the air reactor bed is kept on 12 m^3/h. The N_2 stream flow of the fuel reactor bed is kept on 6 m^3/h. The experiment for chemical-looping gasification (CLG) of biomass is investigated at a fuel reactor temperature varied from 750 to 900 ℃ and a continuous period of 60 h is completed. The effect of the fuel reactor temperature on the performance of chemical-looping gasification (CLG) of biomass is investigated with the oxygen carrier.

3.1　Effect of temperature on both fuel reactor and air reactor

The operation temperature is very important and critical for chemical-looping gasification (CLG) of biomass in the dual fluidized beds. The temperatures of the fuel reactor varied from 750 to 900 ℃ in the tests of this work. The effect of temperature on the gas compositions of the fuel reactor is shown in Figure 2.

The concentration of CH_4 in the flue gas of the fuel reactor is kept at below 10% in the fuel reactor temperature ranging from 750 to 900 ℃. However, CO concentration of the flue gas of the fuel reactor significantly increases with an increase of the fuel reactor temperature until 810 ℃ and then it is maintained around 55%. Correspondingly, CO_2 concentration of the flue gas of the fuel reactor is decreased until 810 ℃, then shows almost stabilized line around 25% ~ 30% between 810 ~ 900 ℃, and finally H_2 concentration reaches the highest at 870 ℃ as shown in Figure 2. As results of endothermic reactions in the fuel reactor; CO and H_2 concentrations are increased with increasing temperature.

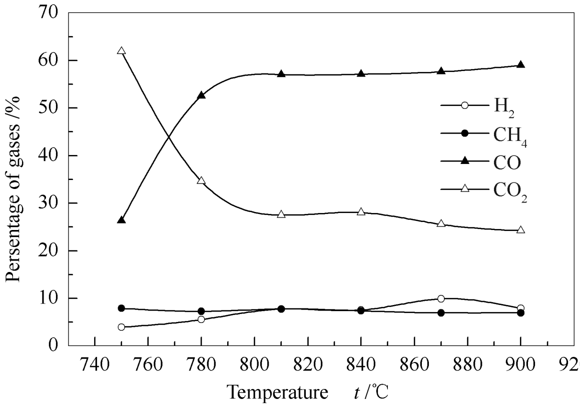

Figure 2 Influence of temperature on the gas concentrations on the fuel reactor

As shown in Figure 3, the flue gas composition of the air reactor affected by the fuel reactor temperature is also tested. The oxygen concentration in the flue gas of the air reactor is maintained around 20.0%, which is the amount of unreacted O_2 from feeded air with oxygen carrier in the air reactor. And N_2 also shows stable line around 75%.

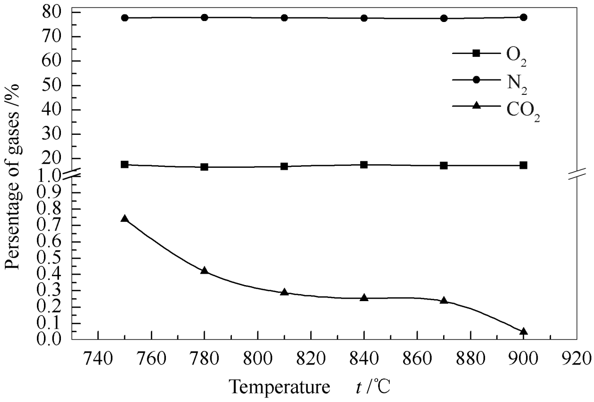

Figure 3 Influence of temperature on the gas concentrations in the air reactor

There are some CO_2 in the flue gas from the air reactor. There can be two reasons for this presence. One is the by-passing of CO_2 gas from the fuel reactor bed to the air reactor bed and the second reason is residual char carried with porous structure of the oxygen carrier from the fuel reactor burnt with hot air in the air reactor bed. The concentration of CO_2 in the flue gas of the air reactor decreases with an increase of the fuel reactor temperature, as illustrated in Figure 3. The chemical looping gasification with biomass in the fuel reactor is highly endorsed by an increase of reaction temperature. The amount of residual char in the fuel reactor decreases with an increase of the fuel reactor temperature. By increasing of the fuel reactor temperature, both the amount of residual char in the fuel reactor and CO_2 concentration of the exit gas from the air reactor are decreased.

The influence of the temperature on the gas selectivity is also investigated, as shown in Figure 4.

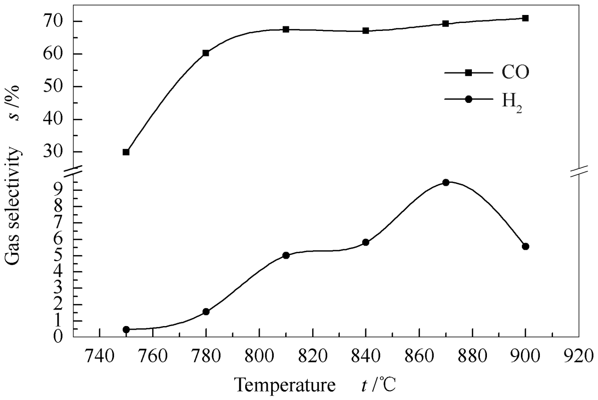

Figure 4 Influence of temperature on the gas selectivity

It shows that carbon conversion rate and gasification efficiency increase with increasing temperature and H_2 production at 870 ℃ reaches the highest rate.

The influence of the temperature on the carbon conversion rate and gasification efficiency also increase with increasing fuel reactor temperature as displayed in Figure 5.

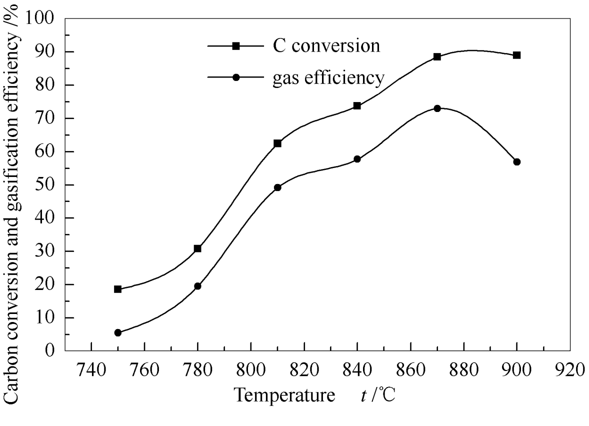

Figure 5 Influence of temperature on the carbon conversion rate and gasification efficiency

The gasification efficiency has showed similar graphs to H_2 as efficiency is decreased with decreasing H_2 productions.

3.2　Oxygen carrier characterization

The air flow of the air reactor bed, N_2 stream of the fuel reactor bed, and biomass feed are stopped after ending of the all experiment procedures. The oxygen carrier particles are collected, sampled and sealed for characterization analysis after cooling of the two reactor beds at room temperature.

3.2.1　X-ray diffraction（XRD）

The fresh and used Fe_2O_3/Al_2O_3-type oxides are examined by XRD to identify the crystalline phases formed. XRD patterns of the fresh, reduced oxides for 20, 40, 60 h cycles are depicted in Figure 6.

As can be seen from the Figure 6, the appearance of the oxygen carrier with the synthesis JCPDS（Joint Committee on Powder Diffraction Standards）card have the best matching standard Fe_2O_3/Al_2O_3 characteristic diffraction peaks. And after 20～60 h cycle peaks and fresh oxygen carrier to obtain a good match oxygen carrier indicating that oxygen carrier after 60 h cycle does not change its crystal form and no chemical change occur in the fuel reactor. It also shows that the Fe_2O_3 phase of the oxygen carrier is completely reduced to Fe_3O_4 phase by biomass syngas in the fuel reactor and then Fe_3O_4 is fully oxidized to Fe_2O_3 in the air reactor. The produced oxygen carriers can be used in a chemical looping gasification of biomass having good reproducibility and stability.

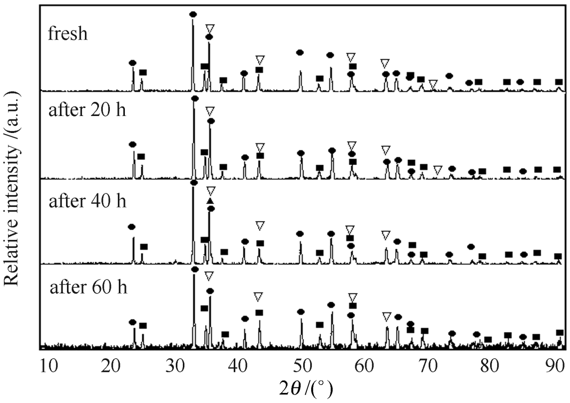

Figure 6　XRD spectra for fresh and used oxygen carrier in a dual circulating fluidized bed unit from the air reactor

●：Fe_2O_3；■：Al_2O_3；▽：Fe_3O_4

3.2.2　SEM micrographs

The micrographs of the fresh and used Fe_2O_3/Al_2O_3 are characterized by SEM. Before（fresh ones）and after 20, 40, 60 h the reacted oxygen carriers pictures are exhibited in Figure 7.

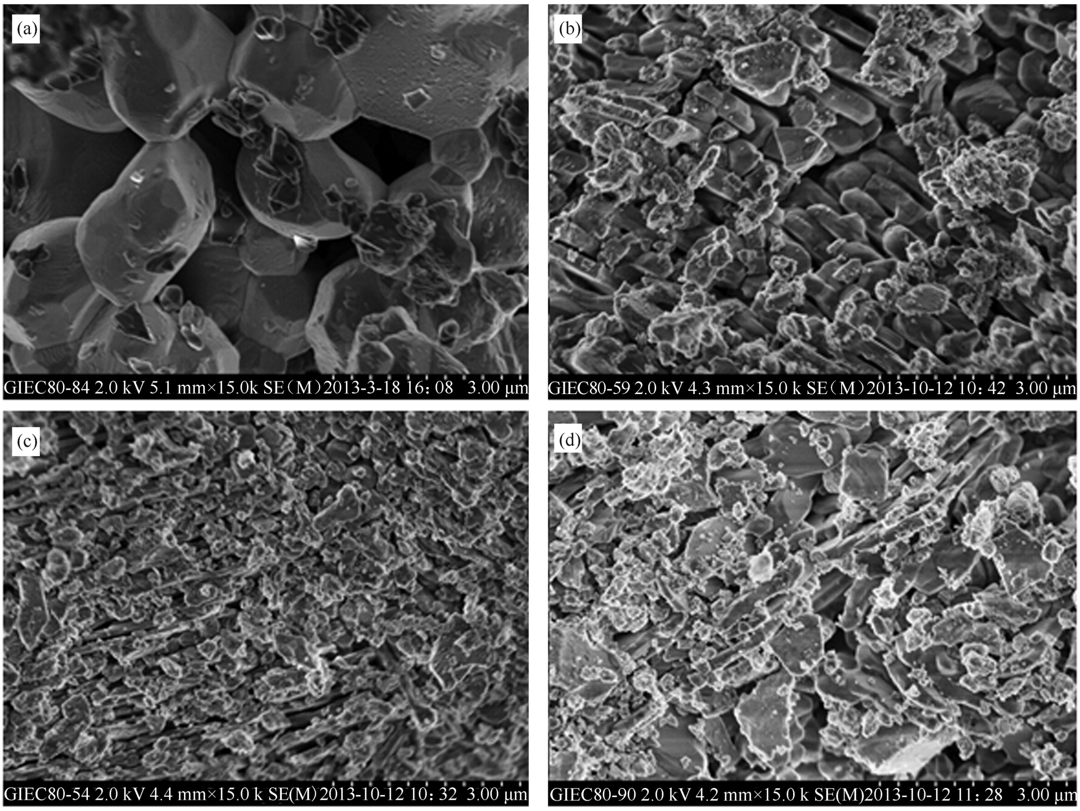

Figure 7　SEM analysis before and after the reaction of oxygen carrier

(a)：fresh；(b)：after 20 h；(c)：after 40 h；(d)：after 60 h

The fresh Fe_2O_3/Al_2O_3 oxygen carrier is about 3 ~ 9 μm in irregular cubes and a gap exists between the porous particles. Al_2O_3 particles as inert support to Fe_2O_3 are distributed in the pores of the particle surface of Fe_2O_3 as can be seen from the electron micrograph in Figure 7(a). After 20 h the reaction cycle Fe_2O_3 oxygen carrier particle size becomes smaller and more orderly arrangement to attach to the aluminum oxide surface. The pores become more structured and the surface area of oxygen carrier increases as shown in Figure 7(b). After 40 h cycle, Oxidative iron particle size is further reduced and the sintering phenomenon is not observed. For the oxygen carrier particles and the biomass, due to multiple air react with the lattice oxygen and molecular oxygen in and out of channel gap, the oxygen carrier particles promote the emergence of a porous shape than further increase the surface area, which helps to promote chemical looping gasification of biomass with oxygen carrier as indicated in Figure 7(c). After 60 h circulating oxygen carrier, part of the particle size is increased, but still maintained a crystalline iron oxide particles as seen in Figure 7(d). The oxygen carrier activity does not decline based on previous experimental results. Compared to BET analysis results show no significant decrease in the specific surface area .

3.2.3 Specific surface area analysis

High internal surface area of the oxygen carrier can help to promote the diffusion and capturizing of molecular oxygen from air in the air reactor and delivering the lattice oxygen in the oxygen carrier in the fuel reactor for fuel reduction and/or decarbonization. Therefore, high specific surface area of produced oxygen carrier is very advantageous for the chemical looping gasification of biomass. The BET method is used for the analysis of the changes in the specific surface area of prepared oxygen carriers after reduction reaction and as a fresh (no used) in this experiment. The results are shown in Table 2. As can be seen from the table, after 20 ~ 60 h of chemical looping gasification for biomass, oxygen carrier surface area and the average pore size are increased. At the first cycle for 20 h they are increased more rapidly and then more slowly, which is consistent with the experimental results of SEM analysis.

Table 2 BET surface area analyses for fresh and used oxygen carriers

Iron-based oxygen carriers	BET-surface area $A/(m^2 \cdot g^{-1})$	Total pore volume $v/(mL \cdot g^{-1})$	Average pore size d/nm
Fresh O. C.	1.727	0.003 8	8.73
After 20 h	2.022	0.006 4	12.02
After 40 h	2.703	0.017 0	25.22
After 60 h	2.767	0.021	30.37

From the BET analysis it is found that the surface area, total pore volume and average pore size of the iron-based oxygen carrier are increased after the reaction in fuel reactor. There is no decreased reactive oxygen carrier and no significant sintering phenomenon. Therefore, the synthesis gas from biomass with the iron-based oxygen carriers has good reaction stability after 60 h cycle reaction. Thus, they can be used as oxygen carrier in biomass chemical looping gasification.

4 Conclusions

In the present study, a novel interconnected fluidized bed device for chemical looping gasification of biomass with man made low cost oxygen carriers is developed. The effect of the reactor temperature on the flue gas composition, gasification efficiency and carbon conversion rate are experimentally investigated. The characterizations of the fresh and used iron-based oxygen carrier are studied by SEM, XRD and BET. The CO and H_2 concentrations are increased relative to the increase of the temperature of the fuel reactor, and CO_2 concentration decreases with the increase of the temperature of both the fuel and air reactor. The H_2 concentration reaches the highest level at 870 ℃. Biomass gasification efficiency and carbon conversion increases accordingly with the increase of the temperature of the fuel reactor. At 900 ℃ gasification efficiency is 78% and carbon conversion efficiency is near to 90%. The feeding rate of biomass in the fuel reactor should match the amount of oxygen carrier circulation. After 60 h the iron-based oxygen carrier does not show polymorph changes with increased surface area. There is no significant sintering and crushing phenomenon. There is no significant decline in the performance of the reduction reaction, indicating that it has good stability and resistance to sintering, and is suitable as a chemical looping gasification of biomass with the iron-based oxygen carrier.

References

[1] RODHE H. A comparison of the contribution of various gases to the greenhouse effect[J]. Science, 1990, **248**(4960): 1217-1219.

[2] MATTISSON T, GARCÍA-LABIANO F, KRONBERGER B, LYNGFELT A, ADÁNEZ J, HOFBAUER H. Chemical-looping combustion using syngas as fuel[J]. Int J Greenh Gas Con, 2007, **1**(2): 158-169.

[3] MATTISSON T, LYNGFELT A, CHO P. The use of iron oxide as an oxygen carrier in chemical-looping combustion of methane with inherent separation of CO_2[J]. Fuel, 2001, **80**(13): 1953-1962.

[4] JOHANSSON M, MATTISSON T, LYNGFELT A, ABAD A. Using continuous and pulse experiments to compare two promising nickel-based oxygen carriers for use in chemical-looping technologies[J]. Fuel, 2008, **87**(6): 988-1001.

[5] RYDEN M, LYNGFELT A, MATTISSON T. Chemical-looping combustion and chemical looping reforming in a circulating fluidized-bed reactor using Ni-based oxygen carriers[J]. Energy Fuels, 2008, **22**(4): 2585-2597.

[6] MATTISSON T, JARDNAS A, LYNGFELT A. Reactivity of some metal oxides supported on alumina with alternating methane and oxygen-application for chemical-looping combustion[J]. Energy Fuels, 2003, **17**(3): 643-651.

[7] BEATRIZ M. CORBELL A, PALACIOS J M. Titania-supported iron oxide as oxygen carrier for chemical-looping combustion of methane [J]. Fuel, 2007, **86**(1/2): 113-122.

[8] LYNGFELT A, LECKNER B, MATTISSON T. A fuidized-bed combustion process with inherent CO_2 separation; application of chemical-looping combustion[J]. Chem Eng Sci, 2001, **56**(10): 3101-3113.

[9] CHUANG S Y, DENNIS J S, HAYHURST A N, SCOTT S A. Development and performance of Cu-based oxygen carriers for chemical-looping combustion[J]. Combust Flame, 2008, **154**(1/2): 109-121.

[10] XUA G W, MURAKAMIA T, SUDA T, MATSUZAW Y, TANI H. Two-stage dual fluidized bed gasification: Its conception and application to biomass[J]. Fuel Process Technol, 2009, **90**: 137-144.

[11] SHEN L H, WU J H, XIAO J. Chemical-looping combustion of biomass in a 10 kW(th) reactor with iron oxide As an oxygen carrie[J]. Energy Fuels, 2009, **23**(5): 2498-2505.

[12] ZHANG Y A, XIAO J, SHEN L H. Simulation of methanol production from biomass gasification in interconnected fluidized beds[J]. Ind Eng Chem Res, 2009, **48**(11): 5351-5359.

[13] ACHARYA B, DUTTA A, BASU P. Chemical-looping gasification of biomass for hydrogen-enriched gas production with in-process carbon dioxide capture[J]. Energy Fuels, 2009, **23**(10): 5077-5083.

[14] XIE Y R, XIAO J, SHEN L H, WANG J, ZHU J, HAO J G. Effects of Ca-based catalysts on biomass gasification with steam in a circulating spout-fluid bed reactor[J]. Energy Fuels, 2010, **24**(5): 3256-3261.

[15] LI F X, ZENG L, FAN L S. Biomass direct chemical looping process: Process simulation[J]. Fuel, 2010, **89**(12): 3773-3784.

[16] GNANAPRAGASAM N V, REDDY B V, ROSEN M A. Opportunities for low-grade coals and biomass for producing hydrogen using iron oxide-based direct chemical looping combustion with effective CO_2 separation[J]. Open Renew Energy J, 2010, **3**: 12-25.

[17] GU H M, SHEN L H, XIAO J, ZHANG S W, SONG T. Chemical looping combustion of biomass/coal with natural iron ore as oxygen carrier in a continuous reactor[J]. Energy Fuels, 2011, **25**: 446-455.

[18] VIRGINIE M, ADANEZ J, COURSON C, DEDIEGO L F, GARCIA-LABIANO F, NIZNANSKY D, KIENNEMANN A, GAYAN P, ABAD A. Effect of Fe-olivine on the tar content during biomass gasification in a dual fluidized bed[J]. Appl Catal B: Environ, 2012, **121-122**(13): 214-222.

[19] SONG T, WU J H, SHEN L H, XIAO J. Experimental investigation on hydrogen production from biomass gasification in interconnected fluidized beds[J]. Biomass Bioenergy, 2012, **36**: 258-267.

[20] MENDIARA T, ABAD A, DEDIEGO L F, GARCIA-LABINO F, GAYAN P, ADANEZ J. Biomass combustion in a CLC system using an iron ore asan oxygen carrier[J]. Int J Greenh Gas Con, 2013, **19**: 322-330.

[21] GU H M, SONG G H, XIAO J, ZHAO H, SHEN L H. Thermodynamic analysis of the biomass-to-synthetic natural gas using chemical looping technology with CaO sorbent[J]. Energy Fuels, 2013, **27**(8): 4695-4704.

[22] GOYAL, H B, SEAL D, SAXENA R C. Bio-fuels from thermo chemical conversion of renewable resources: A review[J]. Renew Sus Energy Rev, 2008, **12**(2): 504-517.

[23] ABAD A, ADANEZ J, GARCIA-LABIANO F, DEDIEGO L, GAYAN P, CELAYA J. Mapping of the range of operational conditions for Cu-, Fe-, and Ni-based oxygen carriers in chemical-looping combustion[J]. Chem Eng Sci, 2007, **62**(1/2): 533-549.

[24] GAO N B, LI A, QUAN C. A novel reforming method for hydrogen production from biomass steam gasification[J]. Bioresour Technol, 2009, **100**(18): 4271-4277.